ANALYSIS OF ATMOSPHERE-EXCITED INTRASEASONAL POLAR MOTION VIA THE TORQUE APPROACH

M. SCHINDELEGGER[1], J. BÖHM[1], D.A. SALSTEIN[2]
[1] Department of Geodesy and Geoinformation, Vienna University of Technology
27-29 Gußhausstraße, A-1040 Wien, Austria
e-mail: michael.schindelegger@tuwien.ac.at, johannes.boehm@tuwien.ac.at,
[2] Atmospheric and Environmental Research, Inc.
131, Hartwell Avenue, Lexington, MA 02421-3126, USA
e-mail: dsalstei@aer.com

ABSTRACT. Alongside the diagnosis of changes in fluid angular momentum, geophysically-driven perturbations of Earth rotation can be investigated by means of interaction torques arising at the boundary of the solid Earth. A recently published reassessment of this modeling route demonstrates the success of investigating torque quantities for the specific purpose of accounting for atmosphere-induced polar motion at intraseasonal periodicities. Here, we expand those considerations by a more detailed analysis of the well-known 10-day atmospheric normal mode signal in polar motion in terms of the underlying driving mechanisms provided by mountain, friction, and equatorial bulge torques. If a fully isostatic response of the sea surface to air pressure variations is implemented, mountain and bulge torque are shown to elicit wobbling motion in the 10-day band at roughly the same level, with the underlying local contributions being dominant over northern hemispheric landmasses. In combination with consistently calculated oceanic angular momentum estimates, atmospheric interaction torques provide a well-closed equatorial excitation budget across the frequency range of 1 to 2 weeks.

1. INTRODUCTION

Small irregularities in Earth rotation associated with motion and mass redistribution effects in the atmosphere, the oceans, the hydrosphere, etc. are preferably inferred from accurate quantifications of angular momentum changes within each of the geophysical fluids. This modeling route is generally viewed as robust and superior to its dynamic complement, the torque approach, which draws on global integrals of the mechanical forces acting on the solid portion of our planet. The strongest torque constituent by far, related to a degree 2/order 1 pressure pattern loading the equatorial bulge, is however common to both approaches in the form of either the ellipsoidal torque or the equatorial mass term of fluid angular momentum. Normal forces and tangential stresses occurring at sloping or along rough topography give rise to secondary but non-negligible mountain and friction torques, respectively, and the local character of these effects is usually cited as a major obstacle in deriving reliable torque-based Earth rotation predictions from global geophysical models. Contrary to this supposition, Schindelegger et al. (2013) recently showed that the quality of present-day atmospheric reanalysis systems has attained a level which renders equatorial torque estimates for the atmosphere as accurate as their AAM (atmospheric angular momentum) counterparts on seasonal and intraseasonal time scales. As a concise follow-up to this study, the present paper is devoted to polar motion variability at retrograde frequencies corresponding to 1–2 weeks, i.e. periodicities that accommodate the prominent atmospheric normal mode ψ_3^1. Feldstein (2008) studied this 10-day, westward propagating wave with regard to its dynamical origin in the atmosphere, concluding that the influence of local torques (mountain + friction) is about five times smaller than the driving provided by the ellipsoidal (equatorial bulge) torque. Here, Feldstein (2008)'s findings shall be complemented by inclusion of oceanic angular momentum (OAM) estimates, which have been corrected for the inverted barometer (IB) response of the oceans to atmospheric pressure fluctuations. This amendment gives a more complete account of the actually observed polar motion signal in the 10-day band.

The investigated daily AAM and torque time series cover the period 2007.0–2010.12 and correspond to those computed by Schindelegger et al. (2013) upon pressure level data (2° horizontal resolution) and surface fields (0.5° resolution) of ERA-Interim, the current reanalysis system of the ECMWF (European Centre for Medium-Range Weather Forecasts). Consistently calculated OAM in terms of non-dimensional

excitation functions were available from the Ocean Model for Circulation and Tides (OMCT) as residual values to an idealized IB ocean. Adhering to this convention, we derived ellipsoidal torque estimates (i.e. AAM mass signals) from an IB-corrected surface pressure field at each epoch.

2. EXCITATION FORMALISM

On time scales of a few days or longer, geophysical excitation embodied by either AAM or atmospheric torques relates to the reported position of the Celestial Intermediate Pole $\hat{p} = p_x - \mathrm{i}p_y$ via (Wahr, 1982)

$$\hat{p} + \frac{\mathrm{i}}{\hat{\sigma}_{cw}}\dot{\hat{p}} = \frac{1}{(C-A)\Omega}\left\{1.12\hat{H}^p + 1.61\hat{H}^w\right\} \tag{1}$$

$$\approx \frac{\mathrm{i}}{(C-A)\Omega^2}\left\{1.12\hat{L}^{e,(s)\to(a)} + 1.61\left(\hat{L}^{m,(s)\to(a)} + \hat{L}^{f,(s)\to(a)}\right)\right\} = \hat{\phi}^e + \hat{\phi}^m + \hat{\phi}^f, \tag{2}$$

where $\hat{\sigma}_{cw}$ is the complex-valued frequency of the Chandler Wobble, A and C denote mean equatorial and axial moments of inertia of the whole Earth which rotates with a nominal angular velocity described by Ω, and $\hat{H}^{p,w}$ represent the standard pressure and wind terms of AAM. Ellipsoidal, mountain and friction torques $\hat{L}^{e,m,f}$ of the atmosphere (a) are understood to act on the solid body (s), and their analytical expressions can be found in Schindelegger et al. (2013), albeit with a reversed sign. $\hat{\phi}^{e,m,f}$ designate the dimensionless excitation functions attributed to each torque component. The apparent equivalence between the pressure term and the ellipsoidal torque $\Omega\hat{H}^p = \mathrm{i}\hat{L}^e$ is exact, while that of the wind term and the cumulative local torque $\Omega\hat{H}^w \approx \mathrm{i}\hat{L}^m + \mathrm{i}\hat{L}^f$ is approximate. An accurate torque-based estimate of $\hat{H}^w$, that might be deployed in the well-established AAM formalism of Eq. (1), is however accessible through integration of the AAM budget equation in the frequency domain, see Schindelegger et al. (2013) for details. If applied to the 10-day band, the pure torque result (Eq. 2) suffers from considerable analytical inadequacies at the level of 10%, specifically due to equating the motion of the Celestial Intermediate Pole to that of the instantaneous rotation axis. It is thus primarily suited for obtaining a qualitative picture of the different torque terms' influence on polar motion.

3. INTRASEASONAL POLAR MOTION AND THE 10-DAY NORMAL MODE

The comparison of observed polar motion (C04-solution of the International Earth Rotation and Reference Systems Service for 2007.0–2010.12) to atmosphere-ocean excitation data was accomplished by aid of Eq. (1) for both angular momentum and torque quantities. After superimposing OAM functions on the right-hand side of the relationship and converting $\hat{L}^e$ to $\hat{H}^p$, the two types of excitation time series differ merely with regard to the wind term $\hat{H}^w$, which stems either from vertical integration of atmospheric fluxes (standard AAM case) or a frequency-dependent scaling of the three torque constituents in the

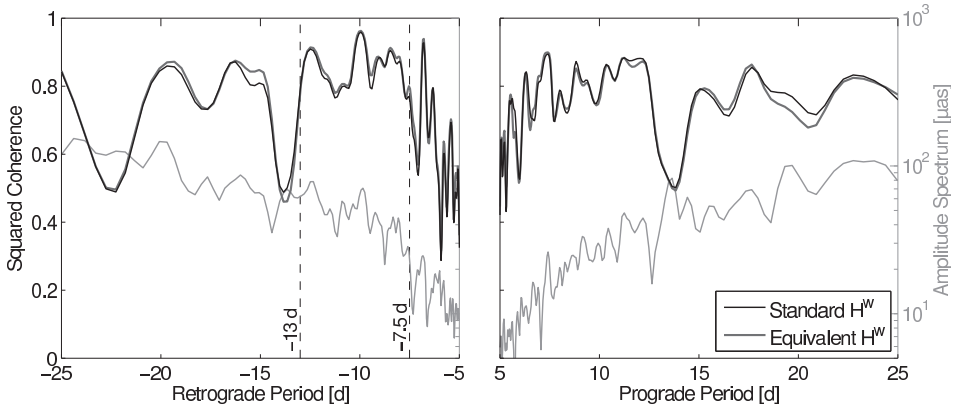

Figure 1: Amplitude spectrum of observed polar motion (*light gray curve*; scale on right) at periodicities from 5 to 25 d, and magnitude-squared coherence values (*black and dark gray curves*; scale on left) between the allocated geodetic excitation and the geophysical excitation as computed from OAM, IB-corrected AAM pressure term, and standard or equivalent AAM wind terms.

discrete spectral space followed by an appropriate inverse transform to the time domain, cf. Schindelegger et al. (2013). This torque-based version of $\hat{H}^w$ has been labeled as *equivalent wind term*. Figure 1 depicts the magnitude-squared coherence spectra between geophysical and geodetic excitation for each of the two approaches and places an amplitude estimate of the reported polar motion in the period range of 5 to 25 d underneath. (The built-in MATLAB functions *mscohere* and *pwelch* were deployed for this purpose.) Coherence values at about 0.7–0.8 on average indicate a close though not ideal match between observed and modeled wobble excitation throughout the probed frequencies, with remaining disparities primarily caused by model inconsistencies and unresolved dynamical processes. Within the 10-day band, whose boundaries were prescribed at -7.5 and -13 d following Feldstein (2008), the amplitude spectrum of up to 80 μas (smoothed value) is enhanced compared to its prograde equivalent. The combined atmosphere-ocean excitation function gives a proper account of the associated signal content as judged from an increased coherence level and generally small phase lag values in the range of $\pm 30°$ (not depicted). Results from the torque-based approach perform marginally better in explaining the observed 10-day wobble and therefore positively warrant further examination of the interaction torques in the context of Earth rotation.

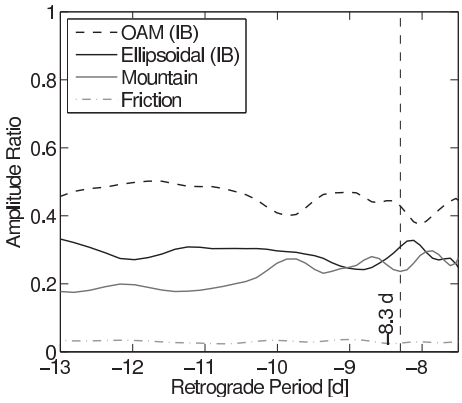

Figure 2: Frequency-dependent ratios of excitation functions for OAM (*black dashed curve*), IB-corrected ellipsoidal torque (*black solid curve*), mountain torque (*gray solid curve*), and friction torque (*gray dot-dashed curve*) relative to the sum of amplitudes of all four components.

Equation (2) is sufficient to qualitatively dissect the total excitation function $\hat{\phi}$ into its individual contributions provided by ellipsoidal, mountain, and friction torques (described by $\hat{\phi}^e$, $\hat{\phi}^m$, and $\hat{\phi}^f$) and the IB-corrected OAM functions as represented by $\hat{\phi}^o$. A smooth picture of the magnitude relationships within the interval (-13;-7.5) d was obtained by splitting the discrete Fourier transform (DFT) coefficients of each excitation component into overlapping spectral segments of distance 0.01 cpd (cycles per day) and bandwidth ± 0.05 cpd. For each sampling frequency σ_i, the DFT values were weighted by a Hanning window, condensed to mean amplitude values $\left|\hat{\phi}^{e,m,f,o}(\sigma_i)\right|$ within the segment, and finally expressed as *amplitude ratios* with respect to $\left|\hat{\phi}^e(\sigma_i)\right| + \left|\hat{\phi}^m(\sigma_i)\right| + \left|\hat{\phi}^f(\sigma_i)\right| + \left|\hat{\phi}^o(\sigma_i)\right|$ (the sum of all four ratios at σ_i amounts to 1, accordingly). Figure 2 displays the constellation of amplitude ratios within the 10-day band, where the usually cited theoretical period of ψ_3^1 at -8.3 d has been specifically marked. Noting that the utilized OAM values express departures from an ideal IB behavior, an approximate equipartition of power between atmospheric and oceanic dynamical processes in $\hat{\phi}$ is readily apparent. This magnitude relationship is in rough agreement with the findings of Ponte and Ali (2002) but probably more reliable in light of the improved geophysical fluid models used in the present study. Moreover, ellipsoidal and mountain torques elicit polar motion variability at approximately the same level (20–30% amplitude ratio each), which contrasts to Feldstein (2008)'s assessment of a much more dominant bulge effect. Both assertions are valid, though, since the IB-correction in the present study absorbs the majority of signal content in $\hat{\phi}^e$. The driving associated with friction torques does not exceed 4% in terms of amplitude ratios, but still constitutes a non-negligible quantity for high-accuracy polar motion considerations.

In a final processing step, the illustrative potential of the torque approach was exploited by a regional analysis of the Earth-atmosphere interaction signals that underlie the large ellipsoidal and mountain

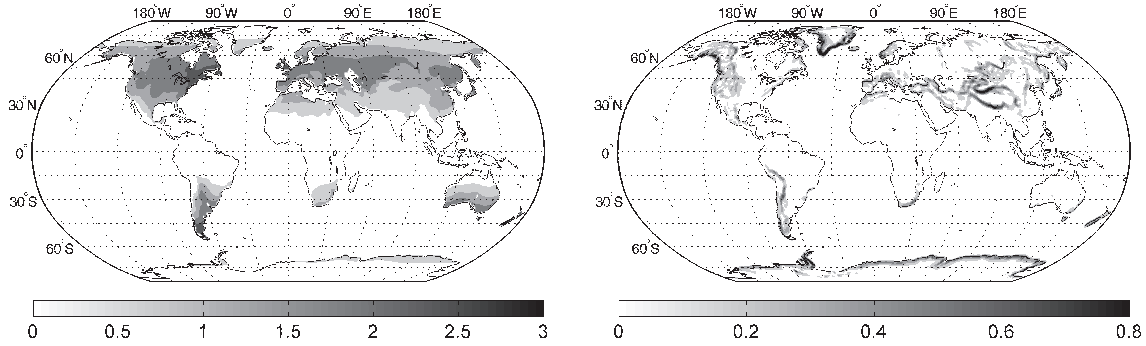

Figure 3: Mean amplitude maps of the grid point-wise contributions to ellipsoidal torque (left panel) and mountain torque (right panel) in the interval of (-13;-7.5) d in units of 10^{16} kgm^{2}s^{-2}.

torque influence on $\hat{\phi}^e$. Specifically, the complete 4-year records of IB and non-IB surface pressure fields from ERA-Interim were converted to grid point-wise contributions to $\hat{L}^e$ (IB) and $\hat{L}^m$ (non-IB, but restricted to land areas in any case) by evaluating their computational expressions (see Schindelegger et al., 2013) except for the double summation over latitude and longitude. The resulting complex-valued grids were subject to bandpass-filtering in the interval (-13;-7.5) d and averaged to mean amplitude values for each cell, leading to the global maps in Figure 3. Regions of angular momentum exchange are apparently confined to midlatitudes, which is intelligible given the spatial pattern of the 10-day normal mode (Feldstein, 2008) as well as the sensitivity areas of polar motion. The IB-correction effectively removes the contributions of pelagic points to $\hat{L}^e$, which is mostly affected by strong but possibly compensating surface pressure values over North America, Eurasia, and Patagonia. Mountain torque signals are of much more local character, with peak amplitudes being present at steep topographic gradients enclosing Greenland, the Tibetan Plateau, and the Antarctic Peninsula.

4. CONCLUSIONS

The dynamics of intraseasonal polar motion in the vicinity of the 10-day atmospheric normal mode have been reassessed on the basis of a recently produced 4-year set of Earth-atmosphere interaction torques and consistently calculated OAM functions. To derive accurate predictions of geophysically excited polar motion and simultaneously retain the torque terms' expressiveness in highlighting the underlying angular momentum exchange, a two-fold mathematical formalism has been compiled and successfully tested. The main findings comprise an equipartition of power between atmospheric and oceanic driving agents of retrograde 10-day wobbles as well as a comparable influence of equatorial bulge and mountain torques on the total atmospheric excitation function–both results of which have been deduced under the assumption of an isostatic oceanic response to air pressure variations. Examination of other prominent modes in both polar motion and changes in length-of-day represents a possible extension to this work.

Acknowledgements. This study was carried out within project P23143-N21 of the Austrian Science Fund. David Salstein was supported by the US National Science Foundation under Grant ATM-0913780.

5. REFERENCES

Feldstein S.B., 2008, "The dynamics of atmospherically driven intraseasonal polar motion", J. Atmos. Sci. 65(7), pp. 2290–2307, doi: 10.1175/2007JAS2640.1.

Ponte R.M., Ali A.H., 2002, "Rapid ocean signals in polar motion and length of day", Geophys. Res. Lett. 29(15), pp. 6-1–6-4, doi: 10.1029/2002GL015312.

Schindelegger M., Salstein D., Böhm J., 2013, "Recent estimates of Earth-atmosphere interaction torques and their use in studying polar motion variability", J. Geophys. Res.118(8), pp. 4586–4598.

Wahr J.M., 1982, "The effects of the atmosphere and the oceans on the Earth's wobble - I. Theory", Geophys. J. R. Astron. Soc. 70, pp. 349–372.